ISBN: 978-3-95450-247-9 ISSN: 2673-5490 doi: 10.18429/JACoW-IPAC2024-THPR02

REVISED ERROR SENSITIVITY STUDY FOR THE ESS PROTON LINAC

R. Miyamoto*, M. Eshraqi, S. Johannesson, Y. Levinsen, N. Milas, D. Noll, M. Serluca
ESS ERIC, Lund, Sweden

Abstract

The normal-conducting injector of the superconducting proton linac of the European Spallation Source (ESS) was commissioned in 2023. Commissioning of the superconducting linac is planned by end of 2024, followed by first beam on the spallation target in 2025. One of the prominent challenges in commissioning and operation of high power accelerators, such as the linac of the ESS, is to minimize beam loss to protect its components from excessive activation and potential damage. Sensitivity studies looking at various types of errors were conducted in the past during the design phase for defining requirements and tolerances. With the commissioning of the full linac approaching, a revised error sensitivity study was carried out, and the result is presented in this paper. The aim of the revised study is to better understand the relation between potential error sources and loss patterns.

INTRODUCTION

The European Spallation Source (ESS) [1] is currently under construction and commissioning [2] in Lund, Sweden, and will be a neutron source driven by a superconducting (SC) proton linac. The schematic layout of the linac is shown in Fig. 1. It starts with normal-conducting (NC) structures, including the ion source (IS), low energy beam transport (LEBT), radio frequency quadrupole (RFQ), medium energy beam transport (MEBT), and drift tube linac (DTL) with five tanks. The SC part has three sections with different cavities, spoke cavities, medium-β elliptical cavities, and high-β elliptical cavities, and each section is referred to as spokes (SPK), medium-β linac (MBL), and high-β linac (HBL). After the high energy beam transport (HEBT), the beam is elevated by ~4.5 m in the vertical dogleg of 4 degrees and expanded and rastered in the accelerator-to-target (A2T) section prior to be sent to the target.

Table 1 lists the high-level design parameters of the ESS linac. The energy, peak current, and duty cycle of 2 GeV, 62.5 mA, and 4% make a 5 MW average power. One significant challenge for such a high-power linac is to mitigate beam losses to protect its components from damages and excessive activation. This is particularly the case for the SC part of the linac because of higher beam power and for preserving surface quality of the SC cavities. Error sensitivity studies were performed in the past to confirm that the confidence level of losses, meeting the commonly used criteria of 1 W/m, is sufficiently high ($\gtrsim$99%) [3, 4] and also to study trends of the lost particles [5]. In the past studies, combined effects from all the types of errors were studied. In the revised study presented in this paper, we treated the errors in magnets and RF separately. The reason is to attempt to identify critical lattice parameters for loss mitigation, in preparation for sending beam through the full linac for the first time, which is schedule towards the end of 2024.

* ryoichi.miyamoto@ess.eu

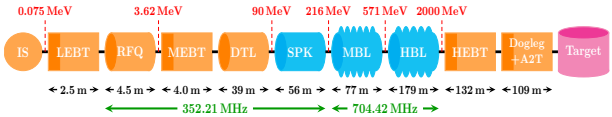

Figure 1: ESS linac design layout.

Table 1: High Level Design Parameters of the ESS Linac

Parameter	Unit	Value
Average beam power	MW	5
Maximum beam energy	GeV	2
Peak beam current	mA	62.5
Beam pulse length	ms	2.86
Beam pulse repetition rate	Hz	14
Duty cycle	%	4
RF frequency	MHz	352.21/704.42

SIMULATION CONDITIONS

Simulations presented in this paper were performed with TraceWin code [6]. In a single run, ~1×10^5 macro-particles were transported from the exit of the RFQ to the target. Table 2 shows selected parameters of the input distribution. For the SC cavities, 3D field-maps were used (a 2D map for the buncher cavities in MEBT), in contrast to the 1D map in the past studies. The number of calculation steps for the field-maps, as well as for the space charge kicks, was 15 per $\beta\lambda$. The meshing for the 3D space charge routine was set to 10×10×10.

Table 3 summarizes the standard set of errors used in this paper. Note that the quadrupoles in the DTL, made of permanent magnets, have different set of values from the rest. The transverse alignment offset of a whole DTL tank was also considered as an additional source for the alignment error of the quadrupoles inside. On the contrary, the alignment errors of the cavities were ignored since they have much less impact on the losses. The field amplitude and phase of each

Table 2: RMS Normalized Emittances (ϵ) and Courant-Snyder Parameters (β and α) of the Input Distribution

Plane	ϵ [π·mm·mrad]	β [m]	α
x	0.253	0.210	−0.052
y	0.252	0.371	−0.310
z	0.361	0.926	−0.481

ISBN: 978-3-95450-247-9 ISSN: 2673-5490 doi: 10.18429/JACoW-IPAC2024-THPR02

Table 3: Standard Quadrupole and Cavity Errors (The symbols are as follows: $\delta B/B$ is the relative field error in a quadrupole, $\delta E/E$ is the relative field amplitude error in a cavity, $\delta\phi$ is the phase error of a cavity, δx and δy are transverse alignment offsets, $\delta\theta_z$ is the tilt around the beam axis, and $\delta\theta_x$ and $\delta\theta_y$ are the tilts around the transverse axes.)

Element	Error	Distribution	Peak/RMS
Quad	$\delta B/B$	Uniform	0.5%
	$\delta x, \delta y$		0.2 mm
	$\delta\theta_z$		0.06°
Quad (DTL)	δB	Uniform	0.5%
	$\delta x, \delta y$		0.1 mm
	$\delta\theta_z$		0.2°
	$\delta\theta_x, \delta\theta_y$		0.5°
DTL tank	$\delta x, \delta y$	Uniform	0.1 mm
Cavity	$\delta E/E$	Gaussian	0.5%
	$\delta\phi$		0.5°

cavity is set experimentally with a process referred to as *phase scan*, where time-of-flight measurements for different amplitudes and phases are compared against the model predictions. In this respect, the errors in the field amplitude and phase represent lumped effects from the error in the phase scan process and manufacturing errors affecting the field profile, and thus affecting the model prediction used in the phase scan. The error values in Table 3 were determined such that each type of error does not cause emittance growth larger than ~10% within a linac section and the 1 W/m criteria is met with a ≳99% confidence level when all the types of errors are considered [3].

As discussed in INTRODUCTION, the cases of the quadrupole errors and cavity errors were studied separately, and the magnitude of the errors were also scanned in steps. Note that, when the quadrupole errors were applied, beam trajectory was corrected, assuming a pessimistic ±0.5 mm error in uniform distributions for all the position measurements. To study all these cases in reasonable time, the number of runs for each case was set to 100, in contrast to 1000 in the past studies. To sample tail cases with the reduced number of runs, the distribution of the cavity errors was switched from the uniform to the Gaussian, compared to the past studies. The distribution of the quadrupole errors was kept to be uniform since the transverse alignment error causes the dominant effect and its distribution is known to be closer to the uniform than the Gaussian.

QUADRUPOLE vs. CAVITY ERRORS

It was seen in the past study that the energy of the particles lost in the SC part of the linac tend to be much lower than the nominal energy of the loss locations [5]. This indicated that the primary causes of these losses were the RF errors. Figure 2 shows the confidence levels of 90%, 95%, and 100% for the losses caused by the quadrupole errors, out of 100

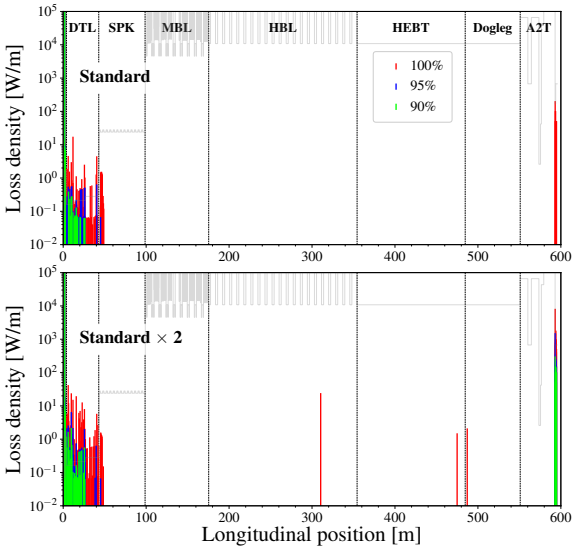

Figure 2: Confidence levels for the losses due to the quadrupole errors. The Gray curve represents aperture.

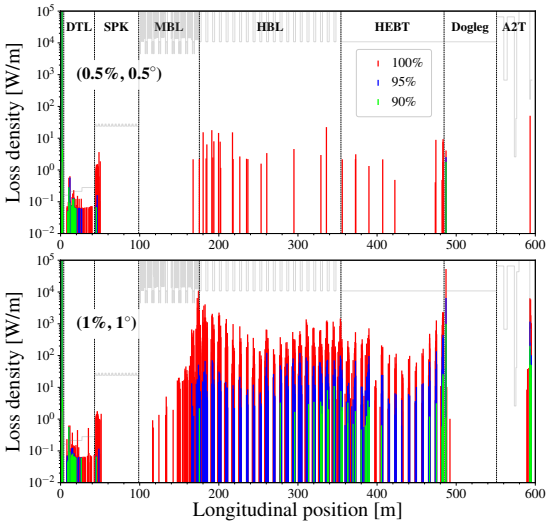

Figure 3: Confidence levels for the losses due to the cavity errors. The Gray curve represents aperture.

runs. The top is for the standard errors from Table 3, and the bottom is for the case with twice errors. As expected, the quadrupole errors are rarely causing losses in the SC part, even for the case with twice errors. It was also re-confirmed that the 1 W/m criteria is met throughout the linac with a ≳95% confidence level. Even the case with twice errors was not too far from the 1 W/m for the 95% level.

Figure 3 shows the confidence levels for the losses due the cavity errors. It is seen that the case with the standard errors (Fig. 3-top) meets the 1 W/m criteria throughout the linac with a ≳95% level. On the other, if the errors are double, the losses in the SC part becomes significantly worse (Fig. 3-top). Hence, for the given set of errors listed in Table 3, the cavity errors are more likely to causes losses in the SC part than the quadrupole errors.

ISBN: 978-3-95450-247-9 ISSN: 2673-5490 doi: 10.18429/JACoW-IPAC2024-THPR02

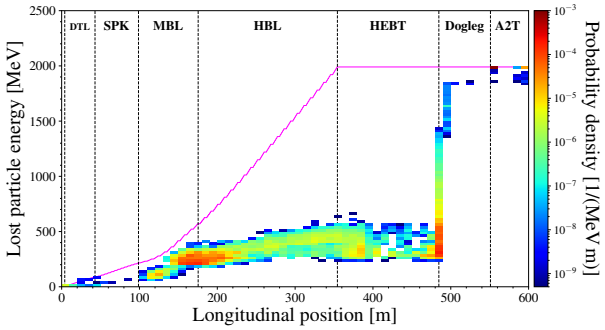

Figure 4: Locations and energies of all the lost particles when the RF errors are enhanced three times. The magenta curve represents the nominal energy.

LOST PARTICLE TRENDS

The previous section saw that the likely cause of losses in the SC part is the cavity errors. Thus, in this section, we see statistical trends of the lost particles caused by the RF errors. The results in the following are from the case when the RF errors are increased by three times. The enhanced error is for improving statistics. Out of 100 runs, ~8.6×10^6 lost particles were generated in total.

Figure 4 shows the locations and energies of all the lost particles. The density is normalized such that the total integration over the position and energy is normalized to one. It is seen that two most likely locations of losses are the vicinity of the MBL-HBL interface and the first bend of the dogleg. For these losses, the energy is peaked around 200-300 MeV. Note that, at the SPK-MBL interface, the RF frequency is doubled from 352 MHz to 704 MHz and the nominal energy of this location is 216 MeV (Fig. 1). Thus, it is likely that the lost particles with $\gtrsim$200 MeV are caused at this location by missing the longitudinal acceptance due to the upstream cavity errors. As seen in Fig. 4, the particles lost in this way could have large correlation distance between the locations of the cause and loss.

Figure 5 shows energy spectra of the lost particles, integrated over each section. The peak energies for the DTL and SPK are much lower than the output energy of the first DTL tank (21 MeV). This indicates that the particles lost in the DTL and SPK are caused by missing the longitudinal acceptance at the DTL entrance. After the SPK, the lost particles are mostly in the energy range of 200-600 MeV.

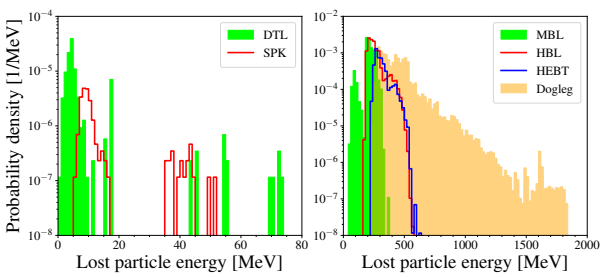

Figure 5: Energy spectra of the lost particles.

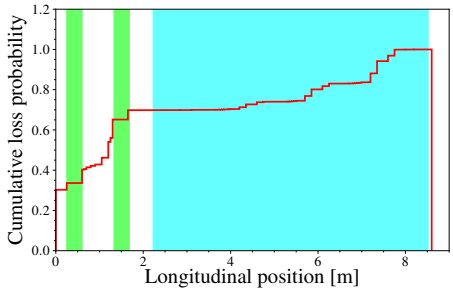

Figure 6: Cumulative loss probability in a lattice period of the MBL and HBL. The quadrupoles and cryomodule are indicated with green and cyan colors.

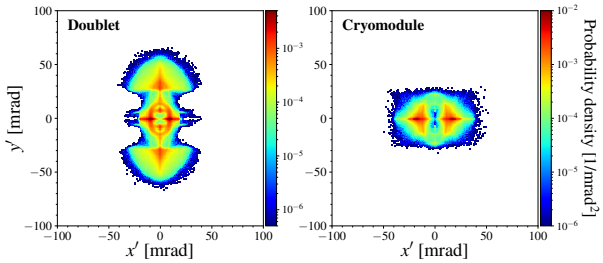

Figure 7: The angular distribution of the lost particles in the MBL and HBL. Left: In the room temperature part including the quadrupoles. Right: In the cryomodules.

Losses with lower energies are seen only in the MBL and those with higher energies are only in the dogleg.

The MBL and HBL share the identical lattice period of ~8.5 m with a room temperature part including a quadrupole doublet and a cryomodule housing four cavities. Figure 6 shows the cumulative loss probability within a period, averaged over all the 9+21 periods in the MBL and HBL. Although the aperture is slightly tighter in the room temperature part, ~30% of losses still occurred inside the cryomodule, mostly in the third and fourth cavities. Figure 7 shows the angular distribution of the particles lost in the MBL and HBL, integrated separately over the room temperature parts (left) and over cryomodules (right). The overall trends for the two cases are very different, but the highest probability is around $|x'|$ ~ 10-20 mrad and $|y'|$ ~ 0 for both cases. These trends for the loss locations and angular distributions will be tested in the real machine with beam loss monitors.

CONCLUSIONS

A revised error sensitivity study was performed for the ESS proton linac in preparation for commissioning of the full linac. It was identified that beam losses in the SC part of the linac are more likely caused by the cavity errors than the quadrupole errors. Observing the energy spectra of the lost particles, the main causes of the losses in our simulations were the particles missing longitudinal acceptance at the entrance of the DTL and MBL. During the upcoming commissioning and initial operations, longitudinal tuning of these two regions will be given extra attention.

ISBN: 978-3-95450-247-9 ISSN: 2673-5490 doi: 10.18429/JACoW-IPAC2024-THPR02

REFERENCES

[1] R. Garoby *et al.*, "The European Spallation Source Design," *Physica Scripta*, vol. 93, no. 1, p. 014 001, 2017. doi:10.1088/1402-4896/aa9bff

[2] R. Miyamoto, "Status and plan of the european spallation source proton linac beam commissioning," English, in *Proc. 14th Int. Particle Accelerator Conf.*, Venice, Italy, May 2023, pp. 2613–2616. doi:10.18429/JACoW-IPAC2023-WEOGB1

[3] M. Eshraqi, R. D. Prisco, R. Miyamoto, E. Sargsyan, and H. Thomsen, "Statistical Error Studies in the ESS Linac," in *Proc. 5th Int. Particle Accelerator Conf. (IPAC'14)*, Dresden, Germany. Jun. 2014, pp. 3323–3325. doi:10.18429/JACoW-IPAC2014-THPME044

[4] R. Miyamoto, M. Eshraqi, and H. D. Thomsen, "An ESS Linac Collimation Study," in *Proc. ICFA Advanced Beam Dynamics Workshop on High-Intensity and High-Brightness Hadron Beams (HB'14)*, East Lansing, MI, USA, Nov. 2015, pp. 62–66. https://jacow.org/HB2014/papers/MOPAB18.pdf

[5] Y. Levinsen, R. D. Prisco, M. Eshraqi, R. Miyamoto, M. Muñoz, and A. Ponton, "Beam Dynamics Challenges in the ESS Linac," in *Proc. ICFA Advanced Beam Dynamics Workshop on High-Intensity and High-Brightness Hadron Beams (HB'16)*, Malmö, Sweden, Jul. 2016, pp. 315–318. doi:10.18429/JACoW-HB2016-TUAM3Y01

[6] D. Uriot and N. Pichoff, "Status of TraceWin Code," in *Proc. 6th Int. Particle Accelerator Conf. (IPAC'15)*, Richmond, VA, USA, May 2015, pp. 92–94. doi:10.18429/JACoW-IPAC2015-MOPWA008